

Quantum measurement of an electron in disordered potential: delocalization versus measurement voltages

Xue-Ning Hu and Xin-Qi Li

*State Key Laboratory for Superlattices and Microstructures, Institute of Semiconductors,
Chinese Academy of Sciences, P.O. Box 912, Beijing 100083, China*

(Dated: September 29, 2018)

Quantum point contact (QPC), one of the typical mesoscopic transport devices, has been suggested to be an efficient detector for quantum measurement. In the context of two-state charge qubit, our previous studies showed that the QPC's measurement back-action cannot be described by the conventional Lindblad quantum master equation. In this work, we study the measurement problem of a multi-state system, say, an electron in disordered potential, subject to the quantum measurement of the mesoscopic detector QPC. The effect of measurement back-action and the detector's readout current are analyzed, where particular attention is focused on some new features and the underlying physics associated with the measurement-induced delocalization versus the measurement voltages.

PACS numbers: 03.67.Lx, 73.23.-b, 85.35.Be

Introduction.— Measurement of an individual quantum state in solid-state system has attracted wide spread attention in recent years, largely due to the promising field of solid-state quantum computation. A possible solid-state implementation of such measurement is to measure a charge qubit by a mesoscopic quantum point contact (QPC) [1, 2]. Very recently, an elegant experiment was performed by employing a QPC to measure the quantum dot occupation by an extra electron, which is further associated with a single electron spin state [3]. This experiment clearly demonstrated the extremely high sensitivity of the QPC detector, implying its possible wide application in the future. It is therefore of importance to develop reliable theoretical description for this important quantum measurement device.

Theoretically, this measurement problem was first studied by Gurvitz [1], followed then by many other groups [2]. Here we mention three typical approaches employed in literatures: (i) the so-called Bloch equation approach developed in Ref. 1 and a number of other papers by Gurvitz *et al*; (ii) the quantum trajectory technique from quantum optics by Goan *et al* [4]; and (iii) the Bayesian approach by Korotkov *et al* [5]. In spite of their different forms in appearance, these three approaches are equivalent in essence. In particular, all of them are based on the same (unconditional) Lindblad master equation. However, as clearly manifested in Ref. 1, the associated Lindblad master equation would result in the *universal* equal occupation probability on the qubit states in stationary state. Obviously, under finite voltages this result breaks down the detailed balance condition, which is thus valid only at high voltage limit.

Very recently, in the context of two-state quantum measurement, we showed that in general (i.e. under arbitrary measurement voltages) the QPC measurement setup cannot be described by the Lindblad master equation [6, 7]. In this work, based on our new treatment

we study the quantum measurement of a *multi-state* system, say, an electron in disordered potential, measured by the mesoscopic detector QPC. It is well known that an electron in disordered potential will be subject to the Anderson localization, and *delocalization* will take place under quantum measurement [8, 9, 10]. In particular, without using any strong projection postulate, Gurvitz showed that *complete delocalization*, i.e., absolute equal occupation probabilities on each local state, will be inevitably approached, under the influence of local measurement by a QPC [11]. There, the delocalization was also interpreted in terms of the measurement-induced loss of quantum coherence. In this work, we show that the delocalization behavior predicted in Ref. 11 is valid only at high voltage limit, and extend the study to arbitrarily finite voltages. Also, we conclude that the delocalization is largely a result of energy exchange of the measured electron with the measurement device QPC, thus depends on the measurement voltages.

Model Description.— As schematically shown in Fig. 1, consider an electron in a one-dimensional array of coupled quantum wells, which is measured by a mesoscopic QPC. The entire system Hamiltonian reads

$$H = H_0 + H', \quad (1a)$$

$$H_0 = H_S + \sum_k (\epsilon_k^L c_k^\dagger c_k + \epsilon_k^R d_k^\dagger d_k), \quad (1b)$$

$$H_S = \sum_{j=1}^N \epsilon_j c_j^\dagger c_j + \sum_{j=1}^{N-1} (\Omega_j c_{j+1}^\dagger c_j + \text{H.c.}), \quad (1c)$$

$$H' = \sum_{k,q} (\Omega_{qk} + \sum_j \chi_{qk}^j c_j^\dagger c_j) c_k^\dagger d_q + \text{H.c.} \quad (1d)$$

In this decomposition, the free part of the total Hamiltonian, H_0 , contains Hamiltonians of the measured system (H_S) and the QPC reservoirs (the last two terms). The operator $c_j^\dagger (c_j)$ corresponds to the creation (annihilation)

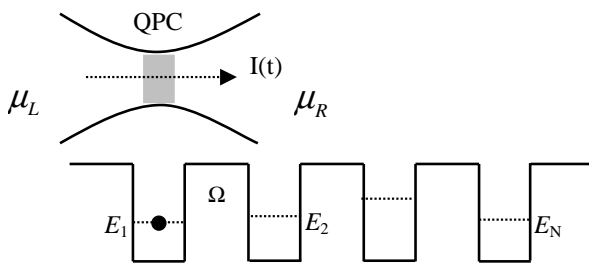


FIG. 1: Schematic illustration of using the mesoscopic quantum-point-contact to measure an electron in multiple coupled quantum wells.

lation) of an electron in the j th well. For simplicity we assume that each well contains a single bound state ϵ_j and is coupled only to its nearest neighbors with couplings Ω_j and Ω_{j-1} . $c_k^\dagger(c_k)$ and $d_k^\dagger(d_k)$ are, respectively, the electron creation (annihilation) operators of the left and right reservoirs of the QPC. The Hamiltonian H' describes electron tunneling between the two reservoirs of the QPC detector with, for instance, tunneling amplitude $\Omega_{qk} + \sum_j \chi_{qk}^j c_j^\dagger c_j$, which generally depends on the measured electron's position that is characterized by occupation operator $c_j^\dagger c_j$. This dependence properly describes the correlation between the detector and the measured system, which enables to draw out measurement information from the output current, and simultaneously propagates back-action of the detector onto the measured system, causing state dephasing and relaxation.

Measurement Back-Action.— Statistically, the measurement back-action onto the measured system is described by a quantum master equation (QME) that is satisfied by the reduced density matrix. Regarding the tunneling Hamiltonian H' as perturbation, the second-order cumulant expansion gives rise to a formal equation for the reduced density matrix [12]

$$\dot{\rho}(t) = -i\mathcal{L}\rho(t) - \int_0^t d\tau \langle \mathcal{L}'(t)\mathcal{G}(t, \tau)\mathcal{L}'(\tau)\mathcal{G}^\dagger(t, \tau) \rangle \rho(t). \quad (2)$$

Here the Liouvillian superoperators are defined as $\mathcal{L}(\dots) \equiv [H_S, \dots]$, $\mathcal{L}'(\dots) \equiv [H', \dots]$, and $\mathcal{G}(t, \tau)(\dots) \equiv G(t, \tau)(\dots)G^\dagger(t, \tau)$ with $G(t, \tau)$ the usual propagator (Green's function) associated with H_S . The reduced density matrix $\rho(t) = \text{Tr}_D[\rho_T(t)]$, resulting from tracing out all the detector degrees of freedom from the entire density matrix. However, for quantum measurement where the specific readout information is likely to be recorded, the average should be performed over the unique class of states of the detector we are trying to keep track of.

For the measurement setup under study, the relevant quantity of readout is the transport current $i(t)$ in the detector, or equivalently, the number of electrons that have tunneled through the detector, $n(t) = \int_0^t dt' i(t')$.

We therefore classify the Hilbert space of the detector as follows. First, we define the subspace in the absence of electron tunneling through the detector as $\mathcal{D}^{(0)}$, which is spanned by the product of all many-particle states of the two isolated reservoirs, formally denoted as $\mathcal{D}^{(0)} \equiv \text{span}\{|\Psi_L\rangle \otimes |\Psi_R\rangle\}$. Then, we introduce the tunneling operator $f^\dagger \sim f_{qk}^\dagger = d_q^\dagger c_k$, and denote the Hilbert subspace corresponding to n -electrons tunneled from the left to the right reservoirs as $\mathcal{D}^{(n)} = (f^\dagger)^n \mathcal{D}^{(0)}$, where $n = 1, 2, \dots$. The entire Hilbert space of the detector is $\mathcal{D} = \bigoplus_n \mathcal{D}^{(n)}$.

With the above classification of the detector states, the average over states in \mathcal{D} in Eq. (2) is replaced with states in the subspace $\mathcal{D}^{(n)}$. Following Ref. 7, a *conditional* master equation can be derived as

$$\begin{aligned} \dot{\rho}^{(n)} = & -i\mathcal{L}\rho^{(n)} - \frac{1}{2} \left\{ [Q\tilde{Q}\rho^{(n)} + \text{H.c.}] \right. \\ & - [\tilde{Q}^{(-)}\rho^{(n-1)}Q + \text{H.c.}] \\ & \left. - [\tilde{Q}^{(+)}\rho^{(n+1)}Q + \text{H.c.}] \right\}. \end{aligned} \quad (3)$$

Here $Q \equiv \Omega_0 + \sum_j \chi_j c_j^\dagger c_j$. For simplicity, we have assumed $\Omega_{qk} = \Omega_0$ and $\chi_{qk}^j = \chi_j$, i.e., the tunneling amplitudes are of reservoir-state independence. Other quantities and notations in Eq. (3) are explained as follows. $\tilde{Q} = \tilde{Q}^{(+)} + \tilde{Q}^{(-)}$, and $\tilde{Q}^{(\pm)} = \tilde{C}^{(\pm)}(\mathcal{L})Q$, with $\tilde{C}^{(\pm)}(\mathcal{L})$ the spectral function of the QPC reservoirs. Under wide-band approximation, $\tilde{C}^{(\pm)}(\mathcal{L})$ can be explicitly carried out as [6]: $\tilde{C}^{(\pm)}(\mathcal{L}) = \eta [x/(1 - e^{-x/T})]_{x=-\mathcal{L}\mp V}$, where $\eta = 2\pi g_{L(R)}$, with $g_{L(R)}$ the density of states of the left (right) reservoir, and T is the temperature. In this work we use the unit system of $\hbar = e = k_B = 1$. The meaning of the super-operator function $\tilde{C}^{(\pm)}(\mathcal{L})$ will become more clear by explicitly carrying out the matrix elements of $\tilde{Q}^{(\pm)}$. In the eigen-state basis $\{|E_m\rangle\}$, we easily obtain $\tilde{Q}_{mn}^{(\pm)} = \tilde{C}^{(\pm)}(\pm\omega_{mn})Q_{mn}$, where $\omega_{mn} = E_m - E_n$ and $Q_{mn} = \langle E_m | Q | E_n \rangle$. In this derivation, the simple algebra $\langle E_m | \mathcal{L}Q | E_n \rangle = \langle E_m | (H_S Q - Q H_S) | E_n \rangle = (E_m - E_n)Q_{mn}$ has been used. Here we see clearly that the Liouvillian operator “ \mathcal{L} ” in $\tilde{C}^{(\pm)}(\mathcal{L})$ properly involves the energy transfer between the detector and the measured system into the transition rates, thus implies a detailed balance condition which determines the stationary occupation probabilities.

Note that $\rho^{(n)}(t)$ contains rich information about the measurement. From it, one can obtain the distribution function of tunneled electron numbers, the measurement current, and the output power spectrum, etc. However, the measurement back-action can be described by a much simpler equation, i.e., the *un-conditional* master equation. Summing up Eq. (3) over “ n ”, the unconditional QME satisfied by the reduced density matrix, $\rho = \sum_n \rho^{(n)}$, is obtained as

$$\dot{\rho} = -i\mathcal{L}\rho - \frac{1}{2} [Q, \tilde{Q}\rho - \rho\tilde{Q}^\dagger], \quad (4)$$

where the term $[\dots]$ describes the back-action of the detector on the measured system. At high-voltage limit, i.e., the voltage is much larger than the eigen-energy differences “ ω_{mn} ” as mentioned above, the spectral function $\tilde{C}^{(\pm)}(\mathcal{L}) \simeq C^{(\pm)}(0)$, and Eq. (4) reduces to a Lindblad-type master equation

$$\dot{\rho} = -i\mathcal{L}\rho + \tilde{C}(0) \left[Q\rho Q - \frac{1}{2}(Q^2\rho + \rho Q^2) \right], \quad (5)$$

where $\tilde{C}(0) = \tilde{C}^{(+)}(0) + \tilde{C}^{(-)}(0)$. It is straightforward to check that this equation is nothing but the Lindblad-type master equation used in literature [1, 4, 5].

In the following we first study the measurement induced dephasing behavior in the *low voltage regime*. Numerically, consider $N = 20$ wells with random energy levels (ϵ_j). The coupling strengths between the nearest-neighbor wells are assumed identical, $\Omega_j = \Omega$, and the disorder strength Δ is set to be $\Delta = 0.9\Omega$ in the numerical calculation. For the QPC, we assume $\Omega_{qk} \equiv \Omega_0 = \Omega$, the density of states of the reservoirs $g_L = g_R = 0.5/\Omega$, and the measurement voltage $V = 1.5\Omega$. From the basics of quantum mechanics, dephasing (or interference destruction) is resulted from the effort of distinguishing the superposition components of a quantum state. Therefore, we adopt two models to reveal the measurement induced dephasing. One model corresponds to that the experimenter wants to distinguish the electron’s position in each quantum well. This can be implemented by assuming quantum-well-state-dependent tunneling coefficients through the QPC in terms of $\Omega + \chi_j$, with $\chi_j = \Omega/\sqrt{4 + (j-1)^2}$. Another is the model studied in Ref. 11, in which the experimenter only distinguishes the electron in the first (nearest) well from others, by simply assuming $\chi_j = \Omega/2$ for occupation of the electron in the first well, and $\chi_j = 0$ for other occupations. The resultant faster dephasing behavior from the former model is plotted in Fig. 2(a) and (b), and the slower dephasing from the latter is shown in Fig. 2(c) and (d). As expected, these quite different dephasing rates are consistent with the general quantum measurement principle, i.e., stronger (more careful) observation leading to faster (more complete) dephasing.

Note that in the local well-state representation, the real part of the off-diagonal matrix element does not vanish after sufficient measurement, e.g., see Fig. 2(a). The underlying reason is that the back-action of the present continuous weak measurement plays a role of an *effective thermal bath*, in particular the measurement voltage is equivalent to an *effective temperature* [6]. As a result, the long-time (sufficient) measurement will make the measured state be an *effective thermal state*, leading to zero off-diagonal elements of the density matrix between the eigen-energy states. Thus, in general the density matrix is not diagonal in the alternative quantum-well-state basis, where the *coherence* between the quantum-well-states originates from the superposition components (branch waves) of the same *eigen-energy state*, but not between them. In Ref. 1 and 11, the high voltage limit leads to

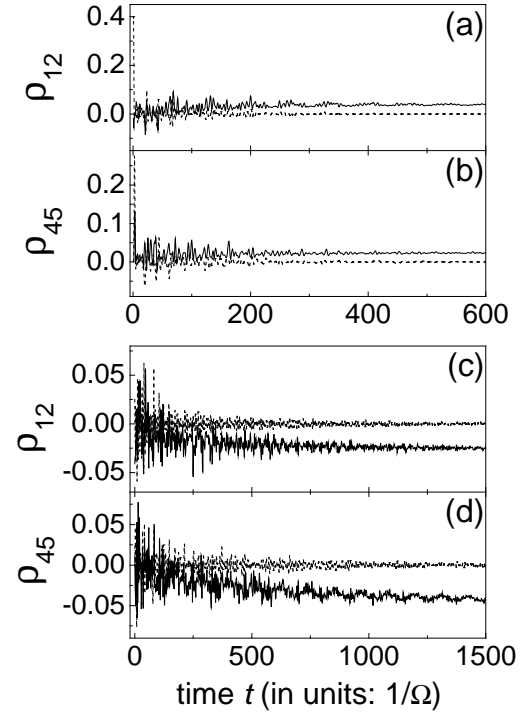


FIG. 2: Measurement-induced dephasing behaviors in the presence of inelastic tunneling through the QPC, in low voltage regime ($V = 1.5\Omega$). Here, by the solid and dashed curves, we plot the real and imaginary parts of the off-diagonal matrix elements ρ_{ij} , which are defined in the local well-state basis. Distinct dephasing rates are obtained from two different models: the faster dephasing behaviors in (a) and (b) correspond to stronger measurement in attempt to distinguish the electron’s position in each quantum well; the much slower ones in (c) and (d) are resulted from observation that only determines the electron in the first (nearest) quantum well.

an equal occupation probability in the effective thermal state, which makes the density matrix be diagonal in arbitrary state basis.

Another consequence of back-action is the measurement-induced relaxation, as numerically shown in Fig. 3, where the adopted parameters are the same as above. Rather than the restriction to the large voltage limit as in Ref. 11, here we particularly focus on the low voltage regime, say, $V < \Delta$, with Δ the disorder strength. Initially (at time $t = 0$), the electron is assumed in the ground state, with a distribution probability dominantly localizing in the eighteenth well, as shown by the solid curves in Fig. 3. As a result of the measurement, the state relaxation gradually takes place, i.e., *delocalization* leads to re-distribution of electron probability in each well. Note that our result shown in Fig. 3(a) differs considerably from that in Fig. 3(b) based on the Lindblad-type master equation Eq. (5). The latter shows that after sufficient relaxation each well is occupied with identical probability, which was indeed

proven *analytically* in Ref. 11. However, our treatment leads to un-equal occupation probabilities in each well. This discrepancy originates from whether the inelastic energy exchange between the detector and the measured system is properly included in the transition rates [6, 7], which leads to a non-trivial detailed balance condition. Remarkably, we notice that ignoring this inelastic effect in the transition rates is equivalent to assuming the large voltage limit. This is in particular illustrated by Fig. 3(c) in comparison with Fig. 3(b).

Output Current.— The un-conditional dynamics described by Eq. (4) appropriately addresses the measurement induced back-action. However, measurement information cannot be drawn out from it. In this sense, the conditional version of master equation (3) contains rich measurement information. Based on it, one can study the readout characteristics of the detector, such as the output noise spectrum and current [7]. Here we exemplify how to calculate the measurement current. From $\rho^{(n)}(t)$, the distribution function reads $P(n, t) = \text{Tr}[\rho^{(n)}(t)]$, which describes the probability of finding “ n ” electrons tunneled through the QPC barrier up to time “ t ”. As a result, the measurement current is obtained as [7]

$$\begin{aligned} I(t) &\equiv e \frac{dN(t)}{dt} = e \sum_n n \text{Tr}[\dot{\rho}^{(n)}(t)] \\ &= \frac{e}{2} \text{Tr}[\bar{Q} \rho Q + \text{H.c.}], \end{aligned} \quad (6)$$

where $\bar{Q} \equiv \tilde{Q}^{(-)} - \tilde{Q}^{(+)}$. In particular, the stationary measurement current can be expressed in general as

$$I_{ss} = I^{(0)} + \tilde{I}. \quad (7)$$

Here $I^{(0)} = \sum_{j=1}^N I_j \rho_{jj}$, with ρ_{jj} the occupation probability of the j th well, and I_j the associated readout current. Explicitly, $I_j = V g_j$, with g_j the conductance defined by $g_j = e^2 \eta (\Omega_0 + \chi_j)^2$. As found in Ref. 6, long-time sufficient measurement only results in complete dephasing between eigenstates, but not the local quantum-well states, i.e., $\rho_{jj'} \neq 0$, which leads to the non-vanishing term \tilde{I} in Eq. (7).

As an explicit example, consider a two-state system (qubit). Let us denote the local energy-level offset by $\epsilon = (\epsilon_2 - \epsilon_1)/2$, and $\Delta = E_2 - E_1 = 2\sqrt{\epsilon^2 + \Omega^2}$ for the eigen-energy difference. For convenience, we also introduce $\sin \theta = 2\Omega/\Delta$. At zero temperature, for low bias voltage $V < \Delta$, the stationary current is $I_{ss} = I_1 \rho_{11} + I_2 \rho_{22} + \frac{\sin \theta}{2} (\chi_1 - \chi_2)^2 \eta V \text{Re} \rho_{12}$. For voltage $V > \Delta$, the current reads $I_{ss} = I_1 \rho_{11} + I_2 \rho_{22} + \frac{\sin \theta}{2} (\chi_1 - \chi_2)^2 \eta \Delta \text{Re} \rho_{12}$. Here, for qubit measurement, we have analytically shown the current “correction” due to the non-vanishing ρ_{12} .

In the following, we study numerically the characteristics of measurement current for more complicated (multi-state) system. To be definite, consider an array of four coupled quantum wells, which is parameterized by $\epsilon_j/\Omega = 2, 4, 1, 0$ ($j=1,2,3,4$). The corresponding eigen-energies read $E_1 = -0.69\Omega$, $E_2 = -1.2\Omega$, $E_3 = 1.83\Omega$,

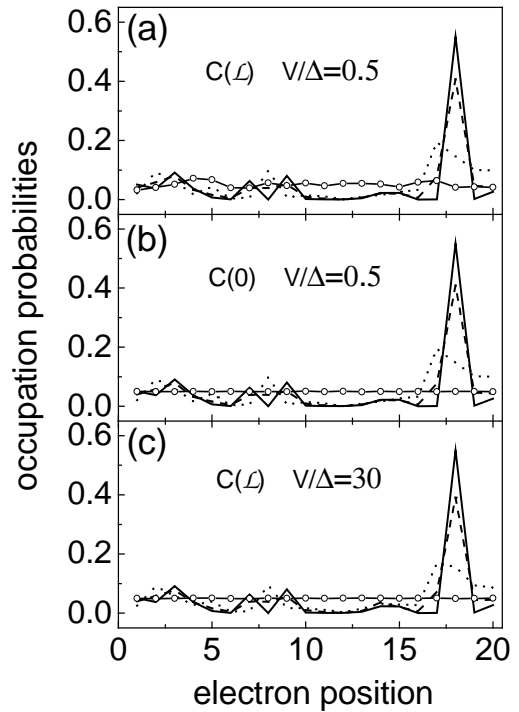


FIG. 3: Measurement-induced delocalization of the electron, initially which is dominantly localized in the eighteenth quantum well (in the ground state), as denoted by the solid curves. Shown in the figure by the dashed, dotted, and symbolized curves are the distribution probabilities in each well, at times $0.4\Omega^{-1}$, $0.8\Omega^{-1}$, and $500\Omega^{-1}$, respectively. In low voltage regime, the detailed-balance preserved result in (a) differs considerably from that in (b) obtained from the Lindblad master equation Eq. (5). At high voltage limit, the result in (c) from Eq. (4) recovers the prediction by Eq. (5).

and $E_4 = 4.67\Omega$. Also, let us denote the eigen-energy differences by $\Delta_{ij} = E_i - E_j$. In Fig. 4(a) we found three transition voltages, $V_1 = 1.9\Omega$, $V_2 = 2.55\Omega$, and $V_3 = 3.5\Omega$, which correspond to, respectively, the transition energies Δ_{21} , Δ_{31} , and Δ_{42} . The conductance plateaus in Fig. 4(a) can be accordingly understood as follows. In the low voltage regime, $V < V_1$, the electron relaxed onto the ground state that contains the dominant components of local well states $|4\rangle$ and $|3\rangle$. The differential conductance is thus approximated by $g_3 \rho_{33} + g_4 \rho_{44}$. In the regime $V_1 < V < V_2$, the detector back-action causes re-excitation of electron from the ground state $|E_1\rangle$ to $|E_2\rangle$, and from $|E_2\rangle$ to $|E_3\rangle$. These processes lead to the obvious changes of occupation probabilities on local states $|4\rangle$ and $|1\rangle$ [Fig. 3(c)], which result in the first conductance plateau in Fig. 3(a). If $V > V_2$, direct excitation from $|E_1\rangle$ to $|E_3\rangle$ takes place, leading to jumps of the local state probabilities ρ_{11} and ρ_{44} as shown in Fig. 3(c), and the second conductance plateau in Fig. 3(a). Finally, as $V > V_3$, excitation from $|E_2\rangle$ to $|E_4\rangle$ is induced by the back-action. As a consequence,

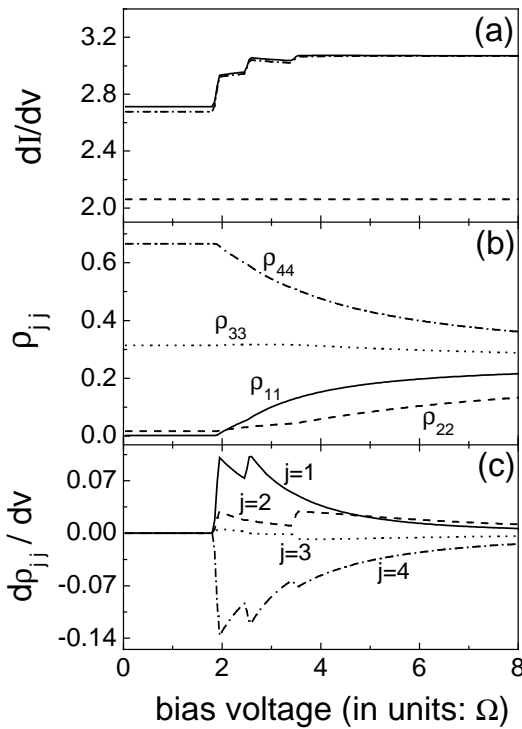


FIG. 4: (a) Measurement current (plotted in terms of the non-linear differential conductance dI/dV) versus the bias voltage across the QPC detector. Here the solid, dot-dashed and dashed curves are, respectively, resulted from “ $I^{(0)} + \tilde{I}$ ”, “ $I^{(0)}$ ” and Gurvitz’s Bloch equation approach [1, 11]. (b) The associated occupation probabilities in the individual local wells, and (c) their differential altering rates with the voltages. Based on (b) and (c) together with the current formula Eq. (7) the conductance plateaus in (a) can be readily understood (see the main text for details).

the occupation probability of the local state $|2\rangle$ has a jump, since $|2\rangle$ is the dominant component of the eigenstate $|E_4\rangle$. This leads to the last observable conductance plateau in Fig. 3(a).

Concluding Remarks.— Based on the detailed-balance preserved Eqs. (3) and (4), we have studied the quantum measurement problem of a multi-state system measured by the mesoscopic QPC detector. The implication of present study is twofold. On one hand, via this multi-state model system, we illustrated that in general the QPC measurement setup cannot be described by the Lindblad-type master equation [i.e. Eq.(5)], which has been commonly assumed (either explicitly or implicitly) in recent literatures [1, 4, 5, 11]. This conclusion may have impact on the future study of solid-state quantum measurement and quantum feedback control. On the other hand, in comparison with previous studies on the measurement-induced delocalization, particularly Ref. 11, we shed new light on the underlying physics. Namely, rather than owing to the mere loss of quantum coherence [11], the delocalization stems largely from the energy exchange of the measured electron with the measurement device QPC, thus depends on the measurement voltages and leads to a number of distinct delocalization features.

Acknowledgments. Support from the National Natural Science Foundation of China, and the Major State Basic Research Project No. G001CB3095 of China are gratefully acknowledged.

[1] S.A. Gurvitz, Phys. Rev. B **56**, 15215 (1997).
[2] I.L. Aleiner, N.S. Wingreen, and Y. Meir, Phys. Rev. Lett. **79**, 3740 (1997); Y. Levinson, Europhys. Lett. **39**, 299 (1997); L. Stodolsky, Phys. Lett. B **459**, 193 (1999); E. Buks, R. Schuster, M. Heiblum, D. Mahalu, and V. Umansky, Nature **391**, 871 (1998); S. Pilgram and M. Büttiker, Phys. Rev. Lett. **89**, 200401 (2002); D. Mozyrsky and I. Martin, Phys. Rev. Lett. **89**, 018301 (2002). S.A. Gurvitz, L. Fedichkin, D. Mozyrsky, and G.P. Berman, Phys. Rev. Lett. **91**, 066801 (2003); A. Shnirman, D. Mozyrsky, and I. Martin, e-print cond-mat/0211618; T.M. Stace and S.D. Barrett, Phys. Rev. Lett. **92**, 136802 (2004); D.V. Averin and A.N. Korotkov, Phys. Rev. Lett. **94**, 069701 (2005); T.M. Stace and S.D. Barrett, Phys. Rev. Lett. **94**, 069702 (2005).
[3] J.M. Elzerman et al., Nature **430**, 431 (2004).
[4] H.S. Goan, G.J. Milburn, H.M. Wiseman, and H.B. Sun, Phys. Rev. B **63**, 125326 (2001); H.S. Goan and G.J. Milburn, Phys. Rev. B **64**, 235307 (2001).
[5] A.N. Korotkov, Phys. Rev. B **60**, 5737 (1999); A.N. Ko-rotkov, Phys. Rev. B **63**, 085312 (2001); A.N. Korotkov and D.V. Averin, Phys. Rev. B **64**, 165310 (2001); R. Ruskov and A.N. Korotkov, e-print cond-mat/0202303.
[6] Xin-Qi Li, Wen-Kai Zhang, Ping Cui, Jiushu Shao, Zhongshui Ma, and Yijing Yan, e-print cond-mat/0309574.
[7] Xin-Qi Li, Ping Cui, and YiJing Yan, Phys. Rev. Lett. **94**, 066803 (2005).
[8] T. Dittrich and R. Graham, Europhys. Lett. **11**, 589 (1990); Phys. Rev. A **42**, 4647 (1990).
[9] P. Facchi, S. Pascazio, and A. Scardicchio, Phys. Rev. Lett. **83**, 61 (1999).
[10] J.C. Flores, Phys. Rev. B **60**, 30 (1999).
[11] S.A. Gurvitz, Phys. Rev. Lett. **85**, 812 (2000).
[12] Y.J. Yan, Phys. Rev. A **58**, 2721 (1998).